

## CHARACTERIZATION OF Nb<sub>3</sub>Sn COATED Nb SAMPLES

Y. Trenikhina\*, S. Posen, FNAL, Fermilab, Batavia, IL, USA  
D. Hall, M. Liepe, Cornell University, Ithaca, USA

### Abstract

Nb<sub>3</sub>Sn has great potential to replace traditional Nb for the fabrication of SRF cavities. The higher critical temperature of Nb<sub>3</sub>Sn potentially allows for an increased operational temperature in SRF cavities, which could save tremendous funding and effort. We present preliminary characterization of a Nb<sub>3</sub>Sn layer grown on flat a Nb sample prepared by the same chemical vapor deposition method that is used for the cavity coating. XRD, SEM, STEM/EDS, TEM imaging and diffraction characterization was used in order to evaluate any chemical and structural defects that could be responsible for the limited quench field and high residual resistance. Variation of local stoichiometry was found in the Nb<sub>3</sub>Sn layer, which is in line with previous studies. Regions of decreased Sn content can have a lower T<sub>c</sub> in comparison to the stoichiometric composition, which may be responsible for the limited performance. AES investigations of the Nb<sub>3</sub>Sn surface after HF-rinse were done in order to explore the mechanism that is responsible for the performance degradation of HF-rinsed Nb<sub>3</sub>Sn coated cavities.

### INTRODUCTION

Growing demand for higher SRF cavity performance at higher accelerating gradients brings traditional niobium to it's theoretical limits. Nb<sub>3</sub>Sn alloy is one of the primary alternative materials for SRF cavity production. Being a type II superconductor with maximum T<sub>c</sub> of 18K and superheating field of 400 mT, Nb<sub>3</sub>Sn offers a much broader parameter space for new SRF performance records. An optimized chemical vapor deposition method adopted at Cornell university for the production of Nb<sub>3</sub>Sn coating on Nb cavities has shown the great potential of Nb<sub>3</sub>Sn for SRF applications. However early quenching and elevated residual resistance were found to limit SRF performance of Nb<sub>3</sub>Sn coated Nb cavities [1].

In order to understand and overcome performance limitations for Nb<sub>3</sub>Sn cavities, intrinsic properties of Nb<sub>3</sub>Sn coating need to be evaluated at microscopic scale. Understanding the connections between Nb<sub>3</sub>Sn material defects and RF performance of the cavities will help to optimize the coating process. Such an optimization could improve the design of the future Nb<sub>3</sub>Sn coating facility at Fermilab [2]. In order to build up a toolset for routine evaluation of Nb<sub>3</sub>Sn coating, structural and chemical evaluation of Nb<sub>3</sub>Sn coated Nb samples was initiated. The samples were prepared at Cornell University by chemical vapor deposition of Sn vapor into Nb surface in the temperature range of 1000C to 1200C [1]. This paper discusses the results of structural and analytical characterization with X-Ray Diffraction (XRD),

Auger Electron Spectroscopy (AES), Scanning Electron Microscopy (SEM), Transmission Electron Microscopy (TEM), Scanning Transmission Electron Microscopy (STEM) and Energy Dispersive Spectroscopy (EDS).

### EXPERIMENTAL METHODS

#### TEM Sample Preparation

Cross sectional TEM samples were prepared from Nb<sub>3</sub>Sn coated Nb flat sample by Focused Ion Beam (FIB) using a Helios 600 FEI instrument at the Materials Research Laboratory (MRL) at the University of Illinois at Urbana-Champaign (UIUC). The FIB lift-out technique allows one to prepare and mount a small rectangular cross sectional sample onto a standard copper TEM half-grid using an Omniprobe micromanipulator. Before FIB milling, the top surface of each cross sectional cut was covered by a protective layer of platinum, in order to protect the native surface from Ga ions.

#### Characterization Techniques

A JEOL JEM 2100 LaB<sub>6</sub> thermionic gun TEM at MRL/UIUC was used for nano-area electron diffraction (NED) and scanning electron nano-area diffraction (SEND). The beam size of approximately 100 nm was used to obtain NED patterns.

The JEM 2010F Schottky FEG TEM at MRL/UIUC operated at 197kV was used for NED and HRTEM imaging. An approximately 80nm sized parallel beam was used to record NED patterns onto the Fuji imaging plates.

A Hitachi HD 2300 Dual EDS STEM at Northwestern University was used for STEM imaging and EDS chemical analysis. STEM images were taken with a high angle annular dark field detector (HAADF) with an incident electron beam energy of 200 kV.

A Pananalytical/Philips X'pert<sup>2</sup> Material Research Diffractometer (with crossed-slit collimator, parallel plates collimator, flat graphite monochromator and proportional detector) at MRL/UIUC was used for XRD. AES was performed with Physical Electronics PHI 660 instrument.

### RESULTS AND DISCUSSION

#### Structural and Chemical Characterization

Two flat Nb<sub>3</sub>Sn coated Nb samples were provided by Cornell University for the material characterization. One of the samples had been anodized at Cornell in order to test the surface composition [3]. Pink-purple oxide which had been grown during the anodization indicated Nb<sub>3</sub>Sn surface under the oxide. Anodized sample had been used for structural and chemical evaluation of the coating.

XRD was initiated to evaluate composition of the sample. As expected, the XRD patten in Fig.1 shows the presence

\* yuliatr@fnal.gov

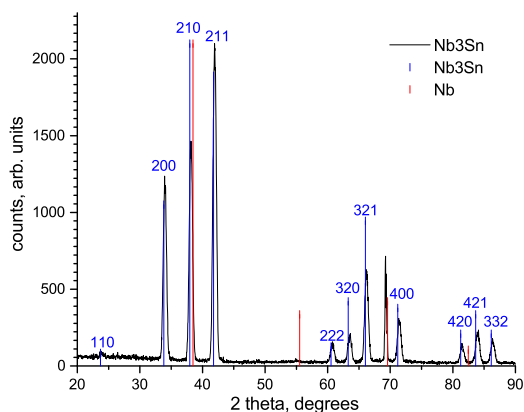


Figure 1: XRD spectra taken from Nb<sub>3</sub>Sn coated Nb sample. Peak indexes for Nb<sub>3</sub>Sn (PDF 00-017-0909) are shown in blue font.

of Nb<sub>3</sub>Sn and Nb due to the relatively large probing depth of this technique. Positions of the reference peaks are indicated by blue and red vertical markers for Nb<sub>3</sub>Sn and Nb, correspondingly. The Nb<sub>3</sub>Sn diffraction pattern closely corresponds to the powder reference file 00-017-0909 [4]. Additional XRD experiments are underway. The Nb pattern shows significant peak intensity variations compared to the reference powder file (00-035-0789) [5] which may be an indication of a preferred orientation of Nb grains.

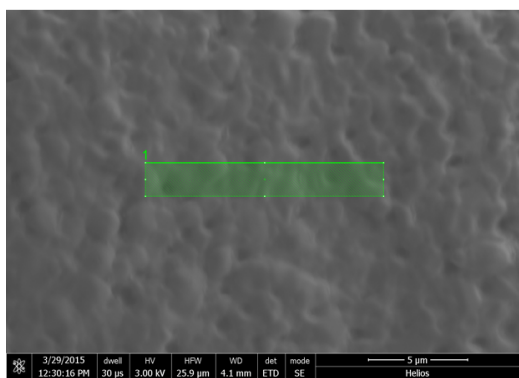


Figure 2: SEM image of Nb<sub>3</sub>Sn surface prior to FIB TEM sample preparation.

SEM image of Nb<sub>3</sub>Sn coated sample surface (Fig.2) shows micron-sized grains. Identical surface morphology was found by the previous studies at Cornell [3].

TEM characterization was used to evaluate structure and composition of the Nb<sub>3</sub>Sn coated Nb sample at microscopic scale. Fig.3 demonstrates a TEM Bright Field (BF) image of the near-surface of a FIB-prepared sample. Thick oxide can be noticed in Fig.3 right underneath the protective Pt layer (top of the image). An approximately 200 nm-thick amorphous oxide layer was grown during the anodization test. Individual grains can be distinguished in the coating layer

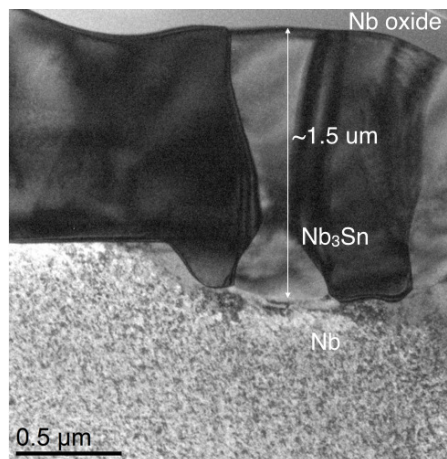


Figure 3: TEM BF image of the near-surface area of Nb<sub>3</sub>Sn coated Nb sample.

which extends for about 1.5 μm below the oxide. Nb<sub>3</sub>Sn coating is followed by the elemental Nb.

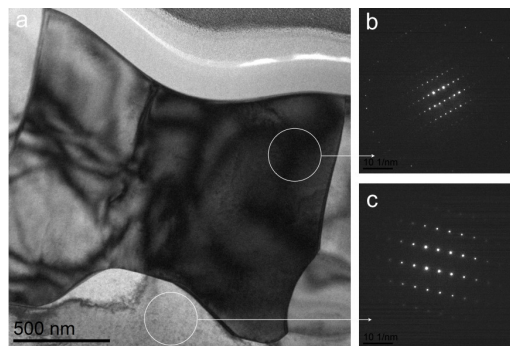


Figure 4: (a) BF image of Nb<sub>3</sub>Sn coated sample's near-surface; (b) NED taken from within Nb<sub>3</sub>Sn grain, [120] Nb<sub>3</sub>Sn zone axis; (c) NED taken below the coating, Nb [113] zone axis.

Local composition of the coating and area below it was checked with NED. Fig.4a shows a BF image of the sample's near-surface when one of the individual Nb<sub>3</sub>Sn grains was tilted to the zone axis. The diffraction pattern taken from within this grain (Fig.4b) shows a Nb<sub>3</sub>Sn single crystal pattern. The NED pattern was indexed according to the [120] Nb<sub>3</sub>Sn zone axis. The NED pattern taken from the area below the coating (fig.4c) shows elemental niobium underneath the coating. The NED pattern in Fig.4c was indexed according to Nb [113] zone axis. Fig.6a shows another individual grain tilted to the zone axis (Fig.6b). The HRTEM image (6c) shows Nb<sub>3</sub>Sn structure on a small scale.

Superconducting properties of Nb<sub>3</sub>Sn strongly depend on stoichiometry. Even a small decrease in Sn content has a great impact on the superconducting transition temperature [6, 7]. In order to directly explore the local elemental composition, STEM/EDS characterization of the FIB-prepared sample was performed. Fig.5a shows a Z-contrast image of the sample's near-surface. EDS maps of Sn and

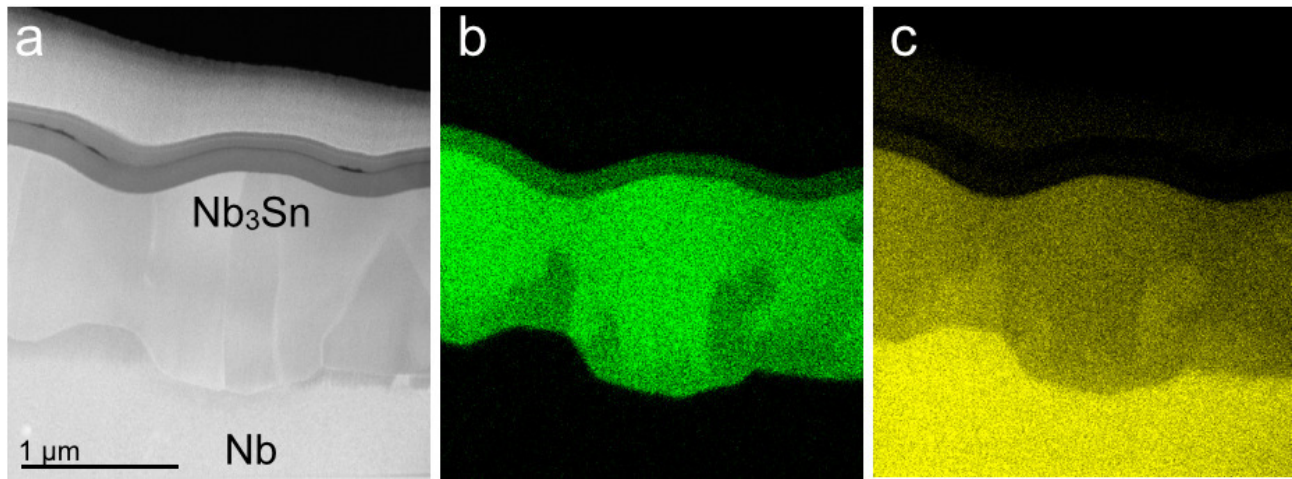


Figure 5: (a) Z-contrast image of the near-surface of the Nb<sub>3</sub>Sn coated Nb sample; (b) EDS map for Sn; (c) EDS map for Nb.

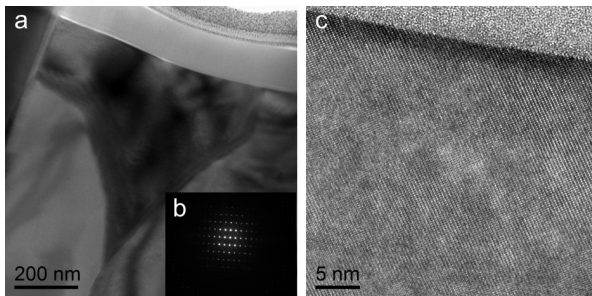


Figure 6: (a) BF image of Nb<sub>3</sub>Sn coated sample's near-surface; (b) diffraction condition for HRTEM image; (c) HRTEM image of the interface of Nb<sub>3</sub>Sn and surface oxide.

Nb distribution in the near-surface are represented in Fig.5b and c, correspondingly. EDS maps were taken with the incident electron energy of 200 kV. Frame time was set to 10s. Map resolution was set to 512 by 384 pixels. The Sn map of the near-surface shows a few areas with decreased intensity of the signal in the Nb<sub>3</sub>Sn coating. Decreased Sn intensity areas are few hundred nm in size and are located close to the interface between Nb<sub>3</sub>Sn and Nb. Decrease in Sn signal intensity in the EDS map can be observed due to either a thinner region of the sample or deficiency of Sn in this particular area. If the thickness variation would be the case, the Nb map would show the same areas of decreased Nb signal intensity. However the Nb map shows brighter regions in Nb<sub>3</sub>Sn coating which indicates higher Nb content. Preliminary estimations of the Sn concentration difference between normal and Sn-deficient areas show the difference of 7 to 8 at.%. Our preliminary STEM/EDS findings are in line with the reported characterization of Nb<sub>3</sub>Sn coated samples produced in Cornell [8]. TEM diffraction investigations are ongoing in order to characterize the local structure of the Sn-deficiency regions.

ISBN 978-3-95450-178-6

710

### Post-HF Rinsing Studies

In the previous studies at Cornell University [1], HF-rinsing of Nb<sub>3</sub>Sn coated cavities induced degraded RF performance. SEM investigation of the cavity/witness sample surface has shown that the Nb<sub>3</sub>Sn surface is covered with some sort of residue particles with various sizes up to 0.5 μm. EDS chemical characterization of the HF-rinse induced residue on Nb<sub>3</sub>Sn surface was not successful due to an indistinguishable EDS signal from the residue particles.

In order to explore the issue of HF-rinse induced residue, we performed AES characterization of the HF-rinsed Nb<sub>3</sub>Sn coated sample. One of the Nb<sub>3</sub>Sn coated samples provided by Cornell went through a few cycles of rinsing with hydrofluoric acid (HF) and ultra pure water. SEM investigations revealed no residue on the surface of the sample following HF-rinsing. AES collected from a few randomly chosen spots on the sample surface did not show the presence of any unusual residue on the sample's surface.

## CONCLUSION

Preliminary structural and analytical characterization of the Nb<sub>3</sub>Sn coated Nb sample demonstrated variation of the local stoichiometry in the Nb<sub>3</sub>Sn layer, which is in line with previous studies [8]. Regions of decreased Sn content can have lower T<sub>c</sub> which could be responsible for the limited RF performance in Nb<sub>3</sub>Sn coated cavities. Additional characterization of the Sn-deficient regions is underway. Evaluation of the Nb<sub>3</sub>Sn coating provided a trial for the characterization toolset which will be routinely used in parallel with the Nb<sub>3</sub>Sn coating facilities at Fermilab.

## REFERENCES

- [1] "Understanding and overcoming limitation mechanisms in Nb<sub>3</sub>Sn superconducting RF cavities", Ph.D. thesis (Cornell University, 2015).

Fundamentals SRF R&D - Other Materials

D02-Non-niobium films

- [2] S. Posen et al., “Fermilab Nb<sub>3</sub>Sn Cavity R&D Program”, TUPB048, *These Proceedings, SRF’15*, Whistler, Canada (2015).
- [3] S. Posen, M. Liepe, “Stoichiometric Nb<sub>3</sub>Sn in first samples coated at Cornell”, SRF 2011, Chicago, THPO066 (2011).
- [4] Powder Diffraction File 00-017-0909. International center for diffraction data, 2005. PDF-2/Release.
- [5] Powder Diffractionfig. File 00-035-0789. International center for diffraction data, 2005. PDF-2/Release.
- [6] H. Devantay, J.L. Jorda, M. Decroux, J. Muller, J. Mater. Sci. 16, 2145 (1981).
- [7] A. Godeke, Supercond. Sci. Technol. 19, R68R80 (2006).
- [8] C. Becker, S. Posen, N. Groll, R. Cook, C. Schleputz, D.L. Hall, M. Liepe, M. Pellin, J. Zasadzinski, T. Proslie, Appl. Phys. Lett. 106, 082602 (2015).